In-Band Coexistence of New Radio with Fixed Satellite Services in C-Band

Amina Girdher[1], Swades De[1], Jun-Bae Seo[2], and Ranjan K. Mallik[1]
[1]Department of Electrical Engineering, Indian Institute of Technology Delhi, New Delhi, India
[2]Department of Artificial Intelligence and Information Eng., Gyeongsang National Univ., Jinju, Republic of Korea

***Abstract*—This paper investigates solutions for seamless in-band coexistence of new radio (NR) network with fixed satellite services (FSS) broadcast network utilizing digital video broadcast-second generation (DVB-S2) technology in the C-band. The in-band coexistence is facilitated by the NR network's adaptability across multiple resource allocation dimensions, including power control, time allocation, and spectral usage within the FSS band. We develop a comprehensive framework for analyzing co-channel interference at both the FSS and NR network receivers, considering their respective transmission and reception characteristics and parameters. We analyze the system performance of the FSS network in terms of Signal-to-Interference-plus-Noise Ratio (SINR). Extensive numerical simulation are conducted to illustrate the impact of system parameters on the in-band coexistence performance. Our results demonstrate that FSS communication has limited impact on the NR network performance. Besides, by judicious choice of spectral and temporal occupancy parameters of NR transmissions, protection distance between NR transmitter and FSS receiver can be significantly reduced without affecting the FSS performance.**

***Index Terms*—C-band, DVB-S2, in-band coexistence, fixed satellite services, new radio**

I. Introduction

The rapid evolution of wireless communication technologies, combined with the growing demand for high-speed data services, has driven the development and implementation of New Radio (NR) systems. However, a key challenge is the limited radio spectrum, which is insufficient to support the growing needs for mobile broadband services. In this context, the reallocation and sharing of spectrum with the existing technologies have become a focal point of regulatory and technical studies worldwide [1].

On one hand, the third Generation Partnership Project (3GPP) Release 18 defines two primary frequency bands for NR: frequency range 1 (FR1) from 410 MHz to 7125 MHz, also known as the sub-6 GHz band, and frequency range 2 (FR2) from 24.25 GHz to 71.0 GHz. On the other hand, fixed satellite services (FSS) are allocated in the frequency band 3.7 GHz to 8 GHz (C-band) in FR1 to support various applications, such as broadcasting, remote sensing, etc. In contrast to FR2 of NR, transmission at C-band offer a significantly broader range and penetration, ensuring consistent and reliable links. This makes the C-band particularly valuable for the coexistence of NR systems with FSS, thereby enabling the possibility of efficient use of radio spectrum.

However, the coexistence of NR system with FSS presents several challenges. The wideband response of commercial low-noise block (LNB) lacks RF filtering, the anticipated high power levels of NR base stations (BSs) surpass the 1 dB compression point of LNBs, leading to saturation and causing the system to operate in a non-linear regime. This non-linear operation significantly impairs the performance of TVRO systems due to the presence of unwanted frequency components within the intermediate frequency band [1]. Thus, the protection of satellite receiving systems of FSS operating in the C-band is crucial while deploying the NR for out-of-band as well as in-band operation.

The International Telecommunication Union (ITU) studied the sharing and compatibility of IMT-Advanced with existing satellite services both in-band as well as in adjacent bands [2], suggesting a minimum required separation distance of FSS ES and the IMT-Advanced BS. A low-cost pass band filter designs as well as 1 dB compression point increment were proposed in [3], [4] to reduce the interference from terrestrial network operating in the adjacent band and avoid non-linearity in ES LNB operation. However, these set of works did not deal with in-band coexistence of NR with the legacy FSS. Further, the study in [5] showed the impact of both out-of-band and in-band interference with respect to the LNB saturation point of the FSS receiver and suggested that beamforming at the 5G BS could mitigate interference and reduce the required protection distance between satellite ES and 5G BS, but it may limit network deployment due to coverage gaps. The authors in [6] developed an analytical framework by using stochastic geometry tools to estimate the aggregated interference to a satellite from coexisting of multiple terrestrial nodes, wherein the power spectral density (PSD) of NR transmitted orthogonal frequency division multiplexing (OFDM) signal was derived and the NR transmitter's in-band and out-of-band spectrum emission masks. However, this approach overestimates interference by not accounting for misalignment between the coexisting parties. The authors in [7], [8] proposed cooperative spectrum sharing techniques that enable multiple networks to efficiently share frequency bands, improving spectrum utilization and reducing interference. However, implementing these techniques necessitates upgrades and dynamic resource adaptation of co-existing networks. Given the extensive deployment of the existing DVB-S2-based FSS broadcast networks, upgrading these FSS networks presents significant challenges.

A. Novelty and Contributions

The protection of satellite receiving systems of FSS operating in the C-band is crucial while deploying the NR network for in-band operation. To accomplish this, accurate co-channel interference analysis at both FSS (particularly the broadcast system using the DVB-S2 technology) and NR network need to be performed. It is observed that the existing works are based on empirical studies that are established on the fact that signal-to-interference plus noise ratio (SINR) must be maintained at an FSS receiver to maintain a desired FSS reception quality. Moreover, the studies in the literature did not exploit various differences between the FSS broadcast and NR transmission technologies, such as the differences in transmitter and receiver characteristics, symbol duration, etc.

Considering the above limitations in the state-of-the-art on in-band coexistence in the FSS (FR1) band, in this paper, we develop a general mathematical framework and

analyse interference on both the FSS and NR receivers, considering their unique system characteristics. The NR utilizes the multi-carrier approach whereas the FSS relies on single-carrier method, leading to fundamental differences in their signal structures. The in-band coexistence between FSS broadcast and NR is enabled by the NR network's flexibility across various dimensions, including power control, time allocation, and spectral usage within the active DVB-S2 band. *To the best of our knowledge, this is first work that considers in-band coexistence of OFDM-based NR system and DVB-S2 based FSS in C-band.*

II. In-Band Coexistent System Model

As shown in Fig. 1, we consider two in-band coexistent communication services: FSS broadcast and NR communication systems. The FSS employs DVB-S2 technology for broadcasting. The FSS broadcast satellite transmitter serves ES TV receiver $\mathrm{U}^{(\mathrm{F})}$ located at $\mathcal{X}_{\mathrm{U}^{(\mathrm{F})}}$ by transmitting multiple channel-per-carrier (MCPC) time division multiplex (TDM) signal. The NR network consists of a BS positioned at $\mathcal{X}_{\mathrm{BS}}$, which serves an NR receiver $\mathrm{U}^{(\mathrm{N})}$ located at $\mathcal{X}_{\mathrm{U}^{(\mathrm{N})}}$. Therefore, we can write the distances of the BS-to-$\mathrm{U}^{(\mathrm{F})}$ and BS-to-$\mathrm{U}^{(\mathrm{N})}$ links as $d_{\mathrm{BF}} = \|\mathcal{X}_{\mathrm{BS}} - \mathcal{X}_{\mathrm{U}^{(\mathrm{F})}}\|$ and $d_{\mathrm{BN}} = \|\mathcal{X}_{\mathrm{BS}} - \mathcal{X}_{\mathrm{U}^{(\mathrm{N})}}\|$ respectively. Further, we consider $f_c^{(\mathrm{F})}$ and $f_c^{(\mathrm{N})}$ be the carrier frequency, and $\mathcal{B}^{(\mathrm{F})}$ and $\mathcal{B}^{(\mathrm{N})}$ be the bandwidth of FSS and NR, respectively. Assuming that the allocated frequency bands of DVB-S2 and NR overlap, i.e. $|f_c^{(\mathrm{F})} - f_c^{(\mathrm{N})}| \leq \left(\mathcal{B}^{(\mathrm{F})} + \mathcal{B}^{(\mathrm{N})}\right)/2$, both systems introduce in-band interference to each other.

A. DVB-S2 Transmission

The MCPC TDM-based DVB-S2 broadcast signal transmiited by the satellite transmitter is given by

$$x^{(\mathrm{F})}(t) = \sqrt{g_T^{(\mathrm{F})} P_T^{(\mathrm{F})}} \sum\nolimits_{k=0}^{K-1} a_k p\left(t - kT^{(\mathrm{F})}\right). \quad (1)$$

Here, $g_T^{(\mathrm{F})}$ is the gain of satellite transmitter, $P_T^{(\mathrm{F})}$ is the transmit power, K is the number of symbols transmitted, a_k is k-th modulated random symbol, and $p(t)$ is the squared Root Raised Cosine (SRRC) filter normalized in energy given by [9]

$$p(t) = \frac{\left[4\alpha\cos\left((1+\alpha)\frac{\pi t}{T^{(\mathrm{F})}}\right) + \sin\left((1-\alpha)\frac{\pi t}{T^{(\mathrm{F})}}\right)\frac{T^{(\mathrm{F})}}{t}\right]}{\pi\sqrt{T^{(\mathrm{F})}}\left[1 - \left(\frac{4\alpha t}{T^{(\mathrm{F})}}\right)^2\right]}, \quad (2)$$

where α is the roll-off factor, $T^{(\mathrm{F})} = 1/\mathcal{R}^{(\mathrm{F})}$ is the symbol period with $\mathcal{R}^{(\mathrm{F})}$ be the symbol rate which is related to satellite transponder's bandwidth as $\mathcal{R}^{(\mathrm{F})} = \mathcal{B}^{(\mathrm{F})}/(1+\alpha)$.

B. NR Transmission

The OFDM signal from the NR BS is given by [10]:

$$x^{(\mathrm{N})}(t) = \frac{\sqrt{g_T^{(\mathrm{N})} P_T^{(\mathrm{N})}}}{\sqrt{T_s^{(\mathrm{N})}}} \sum_{\ell\in\mathbb{Z}}\sum_{n=0}^{N-1} X_n[\ell] e^{\frac{j2\pi n t}{T_s^{(\mathrm{N})}}} \tilde{p}\left(t - \ell T_s^{(\mathrm{N})} + T_g^{(\mathrm{N})}\right), \quad (3)$$

where $g_T^{(\mathrm{N})}$ and $P_T^{(\mathrm{N})}$ are respectively the antenna gain and transmit power of NR BS, N is the number of NR active subcarriers, $T_{tot}^{(\mathrm{N})} = T_s^{(\mathrm{N})} + T_g^{(\mathrm{N})}$ is the total OFDM symbol duration, where $T_s^{(\mathrm{N})}$ is the useful symbol duration and $T_g^{(\mathrm{N})}$ is the guard interval or cyclic prefix duration. $X_n[\ell]$ is the data symbol of the ℓ-th OFDM data block over the n-th NR subcarrier and $\tilde{p}(t) = \prod\left(\frac{t}{T_{tot}^{(\mathrm{N})}}\right)$ is the rectangular pulse shaping function, with $\tilde{p}(t) = 1, 0 \leq t \leq T_{tot}^{(\mathrm{N})}$, and $\tilde{p}(t) = 0$, otherwise.

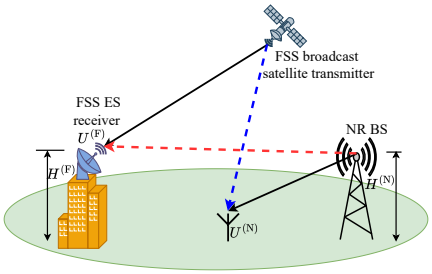

Fig. 1: In-band coexistent FSS and NR system model in C-band.

C. Signal Received at FSS Receiver

The signal received at the input of FSS receiver is given by $y^{(\mathrm{F})}(t) = \sqrt{g_R^{(\mathrm{F})}} s^{(\mathrm{F})}(t) + \sqrt{\hat{g}_R^{(\mathrm{F})}} I^{(\mathrm{F})}(t) + n^{(\mathrm{F})}(t)$, where $s^{(\mathrm{F})}(t)$ is the received desired DVB-S2 signal and $I^{(\mathrm{F})}(t)$ is the received interfering signal from NR BS, and the term $n^{(\mathrm{F})}(t)$ is additive white Gaussian noise (AWGN) at the input of the FSS receiver at the ES. Further, $g_R^{(\mathrm{F})}$ is the on-axis gain of ES antenna in the direction of satellite transponder which is determined from the off-boresight angle, ψ (the angle between the satellite beam axis and direction of the main lobe of ES) following ITU-R F.699-5 model [11] as

$$g_R^{(\mathrm{F})}(\psi) = \begin{cases} g_{max}^{(\mathrm{F})} \ \text{dBi}, & \text{if } 0^\circ < \psi < \psi_{min} \\ 32 - 25\log\psi \ \ \text{dBi}, & \text{if } \psi_{min} \leq \psi < 48^\circ \\ -10 \ \ \text{dBi}, & \text{if } 48^\circ \leq \psi \leq 180^\circ \end{cases} \quad (4)$$

where $g_{max}^{(\mathrm{F})}$ is the main lobe antenna gain. For a given antenna diameter D and operating wavelength λ, ψ_{min} is the minimum boresight. For antenna of diameter $D = 1.8$ m, the main lobe antenna gain $g_{max}^{(\mathrm{F})} = 38$ dBi. Similarly, $\hat{g}_R^{(\mathrm{F})}$ is the off-axis gain of FSS receiver towards the NR signal which can be determined from the off-boresight angle $\widehat{\psi}$ between the NR BS axis and direction of the main lobe of the ES given by

$$\widehat{\psi} = \phi - \tan^{-1}\left(\frac{H^{(\mathrm{N})} - H^{(\mathrm{F})}}{d_{\mathrm{BF}}}\right) \quad (5)$$

where ϕ is the elevation angle of the ES, $H^{(\mathrm{F})}$, and $H^{(\mathrm{N})}$ are the heights of ES and NR BS, respectively.

Further, the DVB-S2 signal $s^{(\mathrm{F})}(t)$ received after undergoing the propagation losses and multipath fading is given by

$$s^{(\mathrm{F})}(t) = e^{j2\pi\Delta f_{\mathrm{off}}^{(\mathrm{F})} t} \sum\nolimits_{i=1}^{L} h_i^{(\mathrm{F})} x^{(\mathrm{F})}\left(t - \tau_i^{(\mathrm{F})}\right) \quad (6)$$

where $f_{\mathrm{off}}^{(\mathrm{F})}$ is the frequency off-set, and $h_i^{(\mathrm{F})}$ and $\tau_i^{(\mathrm{F})}$ are channel coefficient and delay of the i-th path of DVB-S2 channel which contains L paths. Further, the interfering signal from NR BS at the input of ES receiver is given by

$$I^{(\mathrm{F})}(t) = \frac{e^{j2\pi\Delta f_{\mathrm{off}}^{(\mathrm{N})} t}}{\sqrt{T_s^{(\mathrm{N})}}} \sum_{\ell\in\mathbb{Z}}\sum_{n=0}^{N-1}\sum_{j=1}^{L'} X_n[\ell] q_j^{(\mathrm{F})} e^{j2\pi\frac{n}{T_s^{(\mathrm{N})}}\left(t - \tau_j^{(\mathrm{N})} - \theta^{(\mathrm{N})}\right)} \times \tilde{p}\left(t - \tau_j^{(\mathrm{N})} - \ell T_s^{(\mathrm{N})} + T_g^{(\mathrm{N})} - \theta^{(\mathrm{N})}\right), \quad (7)$$

where $\Delta f_{\mathrm{off}}^{(\mathrm{N})}$ is the frequency offset of the received NR signal with respect to DVB-S2 signal, $\tau^{(\mathrm{N})}$ is the delay of the j-th path over NR BS to ES channel which contains L' paths, $q_j^{(\mathrm{F})} = q_{f,j}^{(\mathrm{F})} q_{l,j}^{(\mathrm{F})}$ is the channel coefficient of NR BS to ES link with $q_{f,j}^{(\mathrm{F})}$ being the multipath fading contribution, $q_{l,j}^{(\mathrm{F})}$ is path-loss contribution. Further, $\theta^{(\mathrm{N})}$ is the delay offset

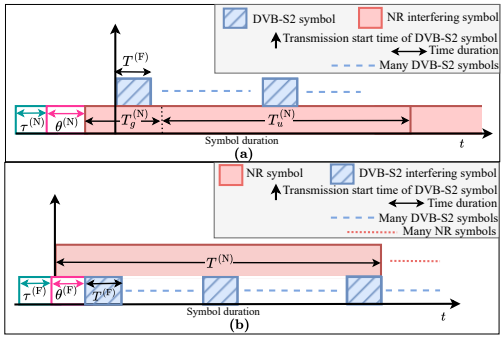

Fig. 2: a) Interference to DVB-S2 symbols by NR symbol; b) Interference to NR symbol by DVB-S2 symbols.

of NR signal with respect to FSS signal due to lack of synchronization.

D. Signal Received at NR Receiver

The signal received at NR receiver is given by

$$y^{(\mathrm{N})}(t) = \sqrt{g_R^{(\mathrm{N})}} s^{(\mathrm{N})}(t) + \sqrt{\hat{g}_R^{(\mathrm{N})}} I^{(\mathrm{N})}(t) + n^{(\mathrm{N})}(t), \quad (8)$$

where $g_R^{(\mathrm{N})}$ is the gain of NR user receiving antenna in the direction of NR BS, $s^{(\mathrm{N})}(t)$ is the desired NR signal, $\hat{g}_R^{(\mathrm{N})}$ is NR user receiver antenna gain in the direction of the satellite transponder, $I^{(\mathrm{N})}(t)$ is the interfering signal from the satellite, and $n^{(\mathrm{N})}(t)$ is AWGN at input of NR receiver with PSD $N_o^{(\mathrm{F})}$.

The NR signal at the input of NR receiver is given by

$$s^{(\mathrm{N})}(t) = \sum_{p=1}^{L'} q_p^{(\mathrm{N})} x^{(\mathrm{N})} \left(t - \tau_p^{(\mathrm{N})}\right), \quad (9)$$

where L' specifies the number multipath components of NR signal, $\tau_p^{(\mathrm{N})}$ is the delay introduced, and $q_p^{(\mathrm{N})}$ is the impulse response of p-th multipath component. At the input of NR receiver, the DVB-S2 signal received after undergoing the multipath fading is given by

$$I^{(\mathrm{N})}(t) = e^{j2\pi\Delta f_{\mathrm{off}}^{(\mathrm{F})} t} \sum_{i=1}^{L} h_i^{(\mathrm{F})} x^{(\mathrm{F})} \left(t - \tau_i^{(\mathrm{F})} - \theta^{(\mathrm{F})}\right), \quad (10)$$

where $\Delta f_{\mathrm{off}}^{(\mathrm{F})}$ is the frequency offset with respect to NR signal, $\theta^{(\mathrm{F})}$ is the delay offset of DVB-S2 signal with respect to NR signal due to lack of synchronization.

E. Channel Model

1) Propagation model for satellite-to-ground link: The satellite-to-ground links are generally influenced by the free space path loss (FSPL), atmospheric absorption, and multipath fading. The overall channel effect can be expressed as $h = h_l h_a h_f$, where h_l is the path loss coefficient, given by $|h_l|^2 = c^2/(4\pi R_E f_c^{(\mathrm{F})})^2$, where c is the speed of light, R_E is the path length in meters. h_f is the multipath fading coefficient that is modelled using Nakagami-m distribution and h_a is atmospheric absorption loss, which is a function of signal carrier frequency, distance traveled, and elevation angle ϕ of the ES receiver. The atmospheric absorption is modelled based on a layered approximation of the atmosphere, as outlined by the ITU [12].

2) Propagation Model for Terrestrial link: The terrestrial links are affected by multipath fading and large-scale fading effects. Thus, the channel coefficient can be expressed as $q = q_f q_l$, where q_f is the multipath fading coefficient which is modelled using Nakagami-m distribution and q_l is the large-scale fading coefficient. The large-scale fading comprises path loss and shadowing effects. Since, the terrestrial links are more susceptible to blockages due to the obstacles in the environment, a probabilistic line-of-sight (LoS) channel model is considered for capturing the path loss effects, where terrestrial links can be modeled as either LoS or non-LoS (NLoS) with certain occurrence probabilities [13]. The probability of having LoS link (denoted by P^{LoS}) for different scenarios (i.e., RMa, UMa, and UMi) with the ground terminal is provided in [13, Table 7.4.2-1]. Then, the overall path loss can be expressed as

$$q_l = P^{\mathrm{LoS}} q_l^{\mathrm{LoS}} + (1 - P^{\mathrm{LoS}}) q_l^{\mathrm{NLoS}}, \quad (11)$$

where q_l^{LoS} and q_l^{NLoS} respectively represent the path loss corresponding to LoS and NLoS.

III. SINR Characterization

A. Analysis of SINR at FSS Receiver

The FSS receiver processes signals using the SRRC matched filter. Its impulse response is given by $p_{MF}(t) = p(T^{(\mathrm{F})} - t)$. Hence, the desired k-th DVB-S2 symbol at the output of matched filter after time synchronization followed by frequency synchronization is expressed as

$$\tilde{a}_k = \sqrt{g_R^{(\mathrm{F})}} \int_0^{T^{(\mathrm{F})}} s^{(\mathrm{F})}(t) p(t) dt = \mathcal{A}_1 H^{(\mathrm{F})} a_k, \quad (12)$$

where $\mathcal{A}_1 = \sqrt{g_T^{(\mathrm{F})} g_R^{(\mathrm{F})} P_T^{(\mathrm{F})}}$ and $H^{(\mathrm{F})} = \sum_{i=1}^{L} h_i^{(\mathrm{F})} \delta(t - \tau^{(\mathrm{F})})$ is the impulse response of the channel.

Similarly, the ES receiver decomposes the NR signal using the SRRC matched filter. Hence, the interference caused by the NR BS on the k-th DVB-S2 symbol is given by

$$I_k = \sqrt{\hat{g}_R^{(\mathrm{F})}} \int_0^{T^{(\mathrm{F})}} I^{(\mathrm{F})}(t) p(t) dt. \quad (13)$$

Based on the data sheets in [14], [15], $\xi = T_s^{(\mathrm{N})}/T^{(\mathrm{F})} \gg 1$, i.e., the symbol duration of NR transmissions is much greater than the DVB-S2 symbol. In order to estimate the NR interference experienced by the FSS receiver, we need to analyze the NR signal seen at the DVB-S2 receiver. Fig. 2(a) illustrates the interference caused by NR over the DVB-S2 signal, where the duration of one NR symbol encompasses several DVB-S2 symbols. Fig. 2(a) shows that from DVB-S2 receiver point of view, the NR signal is delayed by $\theta^{(\mathrm{N})}$ which represents the asynchronism of NR with respect to DVB-S2 symbol. Moreover, due to multipath propagation, multiple copies of an NR symbol are received with delays $\tau_j^{(\mathrm{N})}$, $j \in \mathbb{N}$, as shown in Fig. 2(a). By expressing the NR signal received at the FSS receiver, the following result can be stated.

Lemma 1: The interference from NR BS over the DVB-S2 symbol experienced by the FSS receiver is obtained as

$$I_k = \frac{\mathcal{A}_2}{\sqrt{T_s^{(\mathrm{N})}}} \sum_{\ell \in \mathbb{Z}} \sum_{n=0}^{N-1} \sum_{j=1}^{L'} X_n[\ell] e^{-\frac{j2\pi n \left(\theta^{(\mathrm{N})} + \tau_j^{(\mathrm{N})}\right)}{T_s^{(\mathrm{N})}}} q_j^{(\mathrm{N})} \times \left[\mathcal{I}_1 + \mathcal{I}_2 + \mathcal{I}_3 - \mathcal{I}_4\right], \quad (14)$$

where $\mathcal{A}_2 = \sqrt{g_T^{(\mathrm{N})} \hat{g}_R^{(\mathrm{F})} P_T^{(\mathrm{N})}}$, and $\mathcal{I}_1$ and $\mathcal{I}_2$ can be obtained from (15) by substituting $x = 1$ for which $\mathcal{K}_1 = \left(c_n T^{(\mathrm{F})} + 1 + \alpha\right)/4\alpha$, and $x = 2$ for which $\mathcal{K}_2 = \left(c_n T^{(\mathrm{F})} - \alpha - 1\right)/4\alpha$, respectively. Similarly, $\mathcal{I}_3$ and $\mathcal{I}_4$ can be obtained from (16) by substituting $y = 1$ for

$$\mathcal{I}_x = \frac{\sqrt{T^{(\mathrm{F})}}}{4\pi} e^{-i\pi\mathcal{K}_x} \Big\{ e^{i\pi 2\mathcal{K}_x} \mathrm{Ei}\Big(i\pi\mathcal{K}_x(4\alpha-1)\Big) - \mathrm{Ei}\Big(i\pi\mathcal{K}_x(4\alpha+1)\Big) - \Big[e^{i\pi 2\mathcal{K}_x} \mathrm{Ei}\Big(-i\pi\mathcal{K}_x\Big) - \mathrm{Ei}\Big(i\pi\mathcal{K}_x\Big)\Big]\Big\} \quad (15)$$

$$\mathcal{I}_y = -\frac{T^{(\mathrm{F})}}{16\alpha} e^{-i\pi\mathcal{K}_y} \Big\{ e^{i\pi 2\mathcal{K}_y} \mathrm{Ei}\Big(i\pi\mathcal{K}_y(4\alpha-1)\Big] + \mathrm{Ei}\Big(i\pi\mathcal{K}_y(4\alpha+1)\Big) - \Big[e^{i2\pi\mathcal{K}_y} \mathrm{Ei}\Big(-i\pi\mathcal{K}_y\Big) + \mathrm{Ei}\Big(i\pi\mathcal{K}_y\Big)\Big]\Big\} \quad (16)$$

which $\mathcal{K}_3 = \big(c_n T^{(\mathrm{F})} - \alpha + 1\big)/4\alpha$ and $y = 2$ for which $\mathcal{K}_4 = \big(c_n T^{(\mathrm{F})} + \alpha - 1\big)/4\alpha$, respectively.

Proof: See Appendix A. ∎

Further, the SINR of decoding DVB-S2 signal experienced by FSS receiver is expressed as

$$\Gamma^{(\mathrm{F})} = \frac{\mathcal{A}_1^2 |H^{(\mathrm{F})}|^2}{\mathcal{A}_2^2 \, \mathbb{E}_{X_n[\ell], q_i^{(\mathrm{N})}, \theta^{(\mathrm{N})}} \left[|\tilde{I}_k|^2 \right] + N_o^{(\mathrm{F})} \mathcal{B}^{(\mathrm{F})}}, \quad (17)$$

where $\tilde{I}_k = I_k/\mathcal{A}_2$ and $\mathbb{E}_{X_n[\ell], q_i^{(\mathrm{N})}, \theta^{(\mathrm{N})}} \left[|I_k|^2 \right]$ is the variance of $\tilde{I}_k$ obtained by averaging over $X_n[\ell]$, $q_i^{(\mathrm{N})}$, and $\theta^{(\mathrm{N})}$.

B. Analysis of SINR at NR Receiver

The NR receiver processes the OFDM signals using the basis function. The OFDM decomposition basis function for ℓ-th NR OFDM symbol's n-th sub-carrier is expressed as:

$$\Phi_{n,\ell}^{(\mathrm{N})}(t) = \frac{1}{\sqrt{T_s^{(\mathrm{N})}}} e^{-j2\pi \frac{nt}{T_u^{(\mathrm{N})}}} \prod \left(\frac{t - \ell T_{tot}^{(\mathrm{N})}}{T_s^{(\mathrm{N})}} \right). \quad (18)$$

Hence, the received signal on the n-th subcarrier over the ℓ-th OFDM data block is given by

$$\tilde{X}_n[\ell] = \sqrt{g_R^{(\mathrm{N})}} \int_{\mathbb{R}} s^{(\mathrm{N})}(t) \Phi_{n,\ell}^{(\mathrm{N})} dt = \mathcal{A}_3 X_n[\ell] Q_n^{(\mathrm{N})}[\ell] \quad (19)$$

where $\mathcal{A}_3 = \sqrt{g_T^{(\mathrm{N})} g_R^{(\mathrm{N})} P_T^{(\mathrm{N})}}$ and $Q_n^{(\mathrm{N})}[\ell] = \sum_{p=1}^{L'} q_p^{(\mathrm{N})} e^{\frac{-j2\pi n \tau_p^{(\mathrm{N})}}{T_s^{(\mathrm{N})}}}$.

Further, the NR receiver processes the undesired FSS broadcast signal as

$$I_n[\ell] = \sqrt{\hat{g}_R^{(\mathrm{N})}} \int_{\mathbb{R}} I^{(\mathrm{N})}(t) \Phi_{n,\ell}^{(\mathrm{N})} dt. \quad (20)$$

Fig. 2(b) shows that one NR symbol is interfered by several DVB-S2 symbols. From the NR receiver point of view, $\theta^{(\mathrm{F})}$ represents the asynchronism. Moreover, due to multipath propagation, multiple copies of a DVB-S2 symbol are received with delays $\tau_i^{(\mathrm{F})}$, $i \in \mathbb{N}$. Let b denote the index of the DVB-S2 symbols received during the period $T_s^{(\mathrm{N})}$. Since $T_s^{(\mathrm{N})} \gg T^{(\mathrm{F})}$ (Tables I and II), the number of DVB-S2 symbols interfering over the n-th subcarrier of the ℓ-th NR symbol is $\xi = T_s^{(\mathrm{N})}/T^{(\mathrm{F})}$.

Lemma 2: The interference seen by the NR receiver from the satellite over the n-th NR subcarrier of ℓ-th symbol is obtained as

$$I_n[\ell] = \frac{\mathcal{A}_4}{\sqrt{T_s^{(\mathrm{N})}}} \sum_{b=0}^{\lfloor \xi \rfloor - 1} a_{k+b} \sum_{i=1}^{L} e^{-\frac{j2\pi n \left(\theta^{(\mathrm{F})} + \tau_i^{(\mathrm{F})}\right)}{T^{(\mathrm{F})}}} q_i^{(\mathrm{F})} \times [\mathcal{J}_1 + \mathcal{J}_2 + \mathcal{J}_3 - \mathcal{J}_4] \quad (21)$$

where $\mathcal{A}_4 = \sqrt{g_T^{(\mathrm{F})} \hat{g}_R^{(\mathrm{N})} P_T^{(\mathrm{F})}}$, $\mathcal{J}_1$ and $\mathcal{J}_2$ are respectively defined in (22) and (23). Here, $\mathcal{Q}_1 = d_k T^{(\mathrm{F})} + 1 + \alpha$, $\mathcal{Q}_2 = d_k T^{(\mathrm{F})} - 1 - \alpha$, $\mathcal{Q}_3 = d_k T^{(\mathrm{F})} + 1 - \alpha$, $\mathcal{Q}_4 = d_k T^{(\mathrm{F})} - 1 + \alpha$, $\mathcal{S}_1 = G_k + T^{(\mathrm{F})}/4\alpha$, $\mathcal{S}_2 = G_k - T^{(\mathrm{F})}/4\alpha$, $\mathcal{S}_3 = G_k - T_s^{(\mathrm{N})} + T^{(\mathrm{F})}/4\alpha$, and $\mathcal{S}_4 = G_k - T_s^{(\mathrm{N})} - T^{(\mathrm{F})}/4\alpha$. Further, $\mathcal{J}_3$ and $\mathcal{J}_4$ are given as

$$\mathcal{J}_3 = j/8 e^{-j\pi(1-\alpha)\frac{G_k}{T^{(\mathrm{F})}}} e^{j\pi \frac{\mathcal{S}_1 \mathcal{Q}_3}{T^{(\mathrm{F})}}} (\mathcal{T}_{1,3} + \mathcal{T}_{2,3}), \quad (24)$$

$$\mathcal{J}_4 = j/8 e^{j\pi \frac{\mathcal{S}_1 \mathcal{Q}_3}{T^{(\mathrm{F})}}} (\mathcal{T}_{1,4} + \mathcal{T}_{2,4}). \quad (25)$$

To obtain $\mathcal{J}_3$, and $\mathcal{J}_4$, we need to evaluate $\mathcal{T}_{1,3}$, $\mathcal{T}_{2,3}$, $\mathcal{T}_{1,4}$, and $\mathcal{T}_{2,4}$. The terms $\mathcal{T}_{1,3}$, and $\mathcal{T}_{1,4}$ in $\mathcal{J}_3$, and $\mathcal{J}_4$ are evaluated using $\mathcal{T}_1$ defined in (26). By substituting $\mathcal{G}_1 = d_k T^{(\mathrm{F})} + 1 + \alpha$, and $\mathcal{H}_1 = 1$ in (26), we obtain $\mathcal{T}_{1,3}$, and by substituting $\mathcal{G}_1 = \mathcal{Q}_4$, and $\mathcal{H}_1 = e^{-j\pi(\alpha-1)\frac{G_k}{T}}$ in (26) we obtain $\mathcal{T}_{1,4}$. Similarly, the terms $\mathcal{T}_{2,3}$, and $\mathcal{T}_{2,4}$ in $\mathcal{J}_3$, and $\mathcal{J}_4$ are evaluated using $\mathcal{T}_2$ defined in (27). By substituting $\mathcal{G}_2 = \mathcal{Q}_3$, and $\mathcal{H}_2 = 1$ in (27), we obtain $\mathcal{T}_{2,3}$, and by substituting $\mathcal{G}_2 = \mathcal{Q}_4$, and $\mathcal{H}_2 = e^{-j\pi(1-\alpha)\frac{G_k}{T^{(\mathrm{F})}}}$ in (27) we obtain $\mathcal{T}_{2,4}$.

Proof: See Appendix B. ∎

Furthermore, SINR at the output of NR receiver is given by

$$\Gamma_n^{(\mathrm{N})} = \frac{\mathcal{A}_3^2 \lambda_n |Q_n^{(\mathrm{N})}[\ell]|^2}{\mathbb{E}_{a_k, q_i^{(\mathrm{F})}, \theta^{(\mathrm{F})}} \left[|I_n[\ell]|^2 \right] + N_o^{(\mathrm{N})} \Delta f_n}, \quad (28)$$

where $\lambda_n = \mathbb{E}\left[|X_n[\ell]|^2 \right]$ fraction of power allocated to n-th subcarrier, $\mathbb{E}_{a_k, q_i^{(\mathrm{F})}, \theta^{(\mathrm{F})}} \left[|I_n[\ell]|^2 \right]$ is the variance of interference from satellite average over a_k, $q_i^{(\mathrm{F})}$, and $\theta^{(\mathrm{F})}$. $N_o^{(\mathrm{N})}$ is the noise PSD per NR subcarrier, Δf_n is subcarrier spacing.

TABLE I: FSS System Specifications [14]

Parameter	Value	Parameter	Value
EIRP of FSS transmitter	53.7 dBW	Bandwidth	36 MHz
Diameter of ES antenna	1.8 m	Carrier frequency	3.8 GHz
Height of FSS receiver	5 m	ES elevation angle	74°
Noise temperature	100 K	Roll-off factor, α	0.2

TABLE II: NR System Specifications [15]

Parameter	Value	Parameter	Value
Bandwidth (MHz)	5, 10, 15	Gaurd Interval	16.7 μs
FFT size	512,1024,1536	Subcarrier spacing	15 KHz
Active subcarriers	301, 601, 901	Symbol duration	66.7 μs
Noise PSD	-165 dBm/Hz	BS power	50 W
Receiver sensitivity	-101.7 dBm	Power of subcarrier	0.075 W

IV. Numerical Results

This section presents the numerical results for the considered co-existing FSS and NR networks. Fig. 3(a) illustrates the SINR performance of the FSS network as a function of d_{BF} under RMa and UMi. It can be seen from Fig. 3(a) that the FSS receiver performance is quite sensitive to d_{BF}. Further, a reduction in the number of active subcarriers shows an improvement in the SINR at the DVB-S2 receiver due to the reduction in the spectral overlap between the FSS and NR networks. Consequently, the required protection distance is reduced in both UMi and RMa scenarios. Compared to RMa, the percentage change in the protection distance is significantly smaller for UMi due to the high attenuation of the NR interference signal. Thus, the impact of reducing subcarriers is more predominant in RMa.

$$\mathcal{J}_1=\frac{j\sqrt{T^{(\mathrm{F})}}}{4\pi}e^{-j\pi(1+\alpha)\frac{G_k}{T^{(\mathrm{F})}}}e^{j\pi\frac{\mathcal{S}_1\mathcal{Q}_1}{T^{(\mathrm{F})}}}\left\{e^{-j\pi\frac{\mathcal{Q}_1}{2\alpha}}\left(\mathrm{Ei}\left(-j\pi\frac{\mathcal{S}_3\mathcal{Q}_1}{T^{(\mathrm{F})}}\right)-\mathrm{Ei}\left(-j\pi\frac{\mathcal{S}_1\mathcal{Q}_1}{T^{(\mathrm{F})}}\right)\right)+\mathrm{Ei}\left(-j\pi\frac{\mathcal{S}_2\mathcal{Q}_1}{T^{(\mathrm{F})}}\right)-\mathrm{Ei}\left(-j\pi\frac{\mathcal{S}_4\mathcal{Q}_1}{T^{(\mathrm{F})}}\right)\right\} \quad (22)$$

$$\mathcal{J}_2=\frac{\sqrt{T^{(\mathrm{F})}}}{4\pi}e^{j\pi(1+\alpha)\frac{G_k}{T^{(\mathrm{F})}}}e^{j\pi\frac{\mathcal{S}_1\mathcal{Q}_2}{T^{(\mathrm{F})}}}\left\{e^{-j\pi\frac{\mathcal{Q}_2}{2\alpha}}\mathrm{Ei}\left(-j\pi\frac{\mathcal{S}_3\mathcal{Q}_2}{T^{(\mathrm{F})}}\right)-e^{-j\pi\frac{G_k}{2\alpha}}\mathrm{Ei}\left(-j\pi\frac{\mathcal{S}_1\mathcal{Q}_2}{T^{(\mathrm{F})}}\right)+\mathrm{Ei}\left(-j\pi\frac{\mathcal{S}_2\mathcal{Q}_2}{T^{(\mathrm{F})}}\right)-\mathrm{Ei}\left(-j\pi\frac{\mathcal{S}_4\mathcal{Q}_2}{T^{(\mathrm{F})}}\right)\right\} \quad (23)$$

$$\mathcal{T}_1=\frac{T^{(\mathrm{F})}\mathcal{H}_1}{2\alpha}\left\{\left(1-\frac{4\alpha G_k}{T^{(\mathrm{F})}}\right)e^{-j\pi\frac{\mathcal{Q}_3}{2\alpha}}\left[\mathrm{Ei}\left(-j\pi\frac{\mathcal{S}_3\mathcal{Q}_3}{T^{(\mathrm{F})}}\right)-\mathrm{Ei}\left(-j\pi\frac{\mathcal{S}_1\mathcal{G}_1}{T^{(\mathrm{F})}}\right)\right]-\left(1+\frac{4\alpha G_k}{T^{(\mathrm{F})}}\right)\left[\mathrm{Ei}\left(-j\pi\frac{\mathcal{S}_4\mathcal{Q}_3}{T^{(\mathrm{F})}}\right)-\mathrm{Ei}\left(-j\pi\frac{\mathcal{S}_2\mathcal{G}_1}{T^{(\mathrm{F})}}\right)\right]\right\} \quad (26)$$

$$\mathcal{T}_2=2G_k\mathcal{H}_2\left\{e^{-j\pi\frac{\mathcal{G}_2}{2\alpha}}\left(\mathrm{Ei}\left(-j\pi\frac{\mathcal{S}_3\mathcal{G}_2}{T^{(\mathrm{F})}}\right)-\mathrm{Ei}\left(-j\pi\frac{\mathcal{S}_1\mathcal{Q}_3}{T^{(\mathrm{F})}}\right)\right)-\mathrm{Ei}\left(-j\pi\frac{\mathcal{S}_4\mathcal{Q}_3}{T^{(\mathrm{F})}}\right)+\mathrm{Ei}\left(-j\pi\frac{\mathcal{S}_2\mathcal{Q}_3}{T^{(\mathrm{F})}}\right)\right\} \quad (27)$$

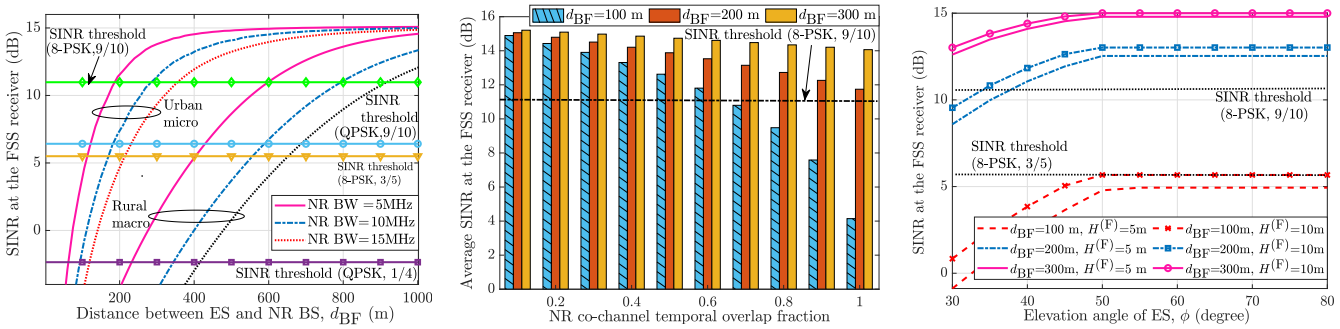

Fig. 3: (a) DVB-S2 performance versus interfering link distance. Allocated power per subcarrier $P_c = 0.055$ W. (b) DVB-S2 performance versus occupied time occupancy fraction under UMi scenario for different d_{BF} when $\mathcal{B}^{(\mathrm{N})} = 5$ MHz, $P_T^{(\mathrm{N})} = 50$ W). (c) DVB-S2 performance versus ϕ under UMi scenario for different d_{BF} and heights of ES $H^{(\mathrm{F})}$ with NR BW $\mathcal{B}^{(\mathrm{N})} = 5$ MHz and NR transmit power $P_T^{(\mathrm{N})} = 50$ W.

In Fig. 3(b), the average SINR at the FSS receiver is observed as a function of temporal overlap fraction, which corresponds to the temporal occupancy of the NR signals. It can be observed from Fig. 3(b) that the SINR performance degrades with an increase in temporal occupancy, as each time slot contributes to the overall interference at the FSS receiver. This observation helps in determining the level of time occupancy at which the SINR of the FSS broadcast signal remains above the predefined threshold. At low time occupancy of NR signal, the SINR of FSS receiver remains above the threshold even when the BS is deployed close to the ES. Thus, required protection distance can be significantly reduced with fewer temporal overlap between the FSS and NR signal transmission.

Fig. 3(c) illustrates the variation of the SINR of FSS broadcasting signal with respect to the elevation angle ϕ of the ES receiver for different values of d_{BF} and ES height $H^{(\mathrm{F})}$ for the UMi scenario. As ϕ increases, the off-boresight angle ($\widehat{\psi}$) increases, leading to a reduction in the off-axis gain of the FSS receiver. Consequently, the NR interference signal is minimized, thereby reducing the impact of interference. Moreover, as the distance between the BS and the ES increases, the gain is further reduced. This is in line with (5) that the increase in distance results in a larger $\widehat{\psi}$, leading to a lower off-axis gain for the FSS receiver. Moreover, it can also be noted from Fig. 3(c) that the impact of ES height is significant when the ES is close to the BR BS due to the strong interference.

Remark 1: *By choosing appropriate transmitter parameters of the in-band coexisting NR transmission, FSS reception quality can be sufficiently ensured without requiring any additional interference mitigation efforts at the FSS ES receiver.*

Fig. 4 represents the variation of received NR signal power with respect to the propagation distance between the NR BS and NR receiver. It is observed that the interference power is much lower than the received NR signal power, and that noise and interference levels are comparable. Thus, it is revealed that that the impact of FSS broadcast is limited on the NR network operating in the same frequency band.

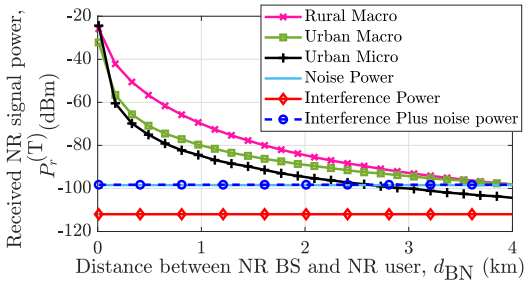

Fig. 4: $P_r^{(\mathrm{T})}$ versus d_{BN} when $\mathcal{B}^{(\mathrm{N})} = 5$ MHz, $P_T^{(\mathrm{N})} = 50$ W.

Remark 2: *The NR receiver antenna gain is generally much smaller than that of the ES receiver. Consequently, the strength of the interfering broadcast FSS signal at a NR receiver from a far away satellite is much lower compared to the signal from the NR BS. This precludes the necessity of employing interference cancellation at the NR receiver.*

V. Conclusion

In this paper, we have studied one-sided in-band coexistence of the NR communication in the vicinity of FSS broadcast receiver operating in C-band. We have derived closed-form expressions for the in-band interference experienced by the TDM-based FSS broadcast network and the OFDM-based NR signal reception quality. The interference analyses at both the FSS and NR receivers have been conducted by considering their respective unique system characteristics. Numerical analysis has revealed that the FSS network has a limited impact on the NR network. The analytical studies on FSS and NR coexistence in this work can be applied to

$$\mathcal{J} = e^{\frac{-j\pi(1+\alpha)G_k}{T^{(\mathrm{F})}}} \int_0^{T_s^{(\mathrm{N})}} \frac{2\alpha (T^{(\mathrm{F})})^{3/2} e^{j\pi t\left(d_k+\frac{(1+\alpha)}{T^{(\mathrm{F})}}\right)}}{\pi\left[(T^{(\mathrm{F})})^2-(4\alpha\,(t-G_k))^2\right]}dt + e^{\frac{j\pi(1+\alpha)G_k}{T^{(\mathrm{F})}}} \int_0^{T_s^{(\mathrm{N})}} \frac{2\alpha (T^{(\mathrm{F})})^{3/2} e^{j\pi t\left(d_k-\frac{(1+\alpha)}{T^{(\mathrm{F})}}\right)}}{\pi\left[(T^{(\mathrm{F})})^2-(4\alpha\,(t-G_k))^2\right]}dt$$
$$+ e^{\frac{-j\pi(1-\alpha)G_k}{T^{(\mathrm{F})}}} \int_0^{T_s^{(\mathrm{N})}} \frac{(T^{(\mathrm{F})})^{5/2}\,(t-G_k)\,e^{j\pi t\left(d_k+\frac{(1-\alpha)}{T^{(\mathrm{F})}}\right)}}{j2t\pi\left[(T^{(\mathrm{F})})^2-(4\alpha\,(t-G_k))^2\right]}dt - e^{\frac{j\pi(1-\alpha)G_k}{T^{(\mathrm{F})}}} \int_0^{T_s^{(\mathrm{N})}} \frac{(T^{(\mathrm{F})})^{5/2}\,(t-G_k)\,e^{j\pi t\left(d_k-\frac{(1-\alpha)}{T^{(\mathrm{F})}}\right)}}{j2t\pi\left[(T^{(\mathrm{F})})^2-(4\alpha\,(t-G_k))^2\right]}dt$$
$$\triangleq \mathcal{J}_1+\mathcal{J}_2+\mathcal{J}_3-\mathcal{J}_4. \tag{B.3}$$

a broader range of scenarios where the interference between TDM and OFDM systems needs to be assessed. Results showed that by choosing appropriate transmitter parameters, the FSS reception quality can be sufficiently ensured without requiring any additional interference mitigation efforts at the FSS ES receiver. Moreover, the strength of interfering broadcast FSS signal at a NR receiver from a far away satellite is much lower compared to the signal from NR BS.

APPENDIX

A. Proof of Lemma 1

The matched filter receiver decomposes the NR signal over N subcarriers of the ℓ-th OFDM block of NR transmitter. Referring to Fig. 2(a), one NR symbol interferes with a current k-th DVB-S2 symbol. Thus, the interference from NR BS on the k-th DVB-S2 symbol can further be expressed by substituting $I^{(\mathrm{F})}(t)$ from (7), $p(t)$ from (2) in (13), and simplifying, we get

$$I_k = \frac{\mathcal{A}_2}{\sqrt{T_s^{(\mathrm{N})}}} \sum_{\ell\in\mathbb{Z}} \sum_{n=0}^{N-1} \sum_{j=1}^{L'} X_n[\ell]\, e^{\frac{-j2\pi n\left(\theta^{(\mathrm{N})}+\tau_j^{(\mathrm{N})}\right)}{T_s^{(\mathrm{N})}}} q_j^{(\mathrm{N})} \mathcal{I}_k, \tag{A.1}$$

where $\mathcal{A}_2 = \sqrt{g_T^{(\mathrm{N})}\,\hat{g}_R^{(\mathrm{F})}\,P_T^{(\mathrm{N})}}$ and $c_n = \Delta f_{\mathrm{off}}^{(\mathrm{N})} + \frac{n}{T_s^{(\mathrm{N})}}$, and

$$\mathcal{I}_k = \int_0^{T^{(\mathrm{F})}} \frac{2\alpha e^{j\pi t\left(c_n+\frac{(1+\alpha)}{T^{(\mathrm{F})}}\right)}}{\pi\sqrt{T^{(\mathrm{F})}}\left[1-\left(\frac{4\alpha t}{T^{(\mathrm{F})}}\right)^2\right]}dt + \int_0^{T^{(\mathrm{F})}} \frac{2\alpha e^{j\pi t\left(c_n-\frac{(1+\alpha)}{T^{(\mathrm{F})}}\right)}}{\pi\sqrt{T^{(\mathrm{F})}}\left[1-\left(\frac{4\alpha t}{T^{(\mathrm{F})}}\right)^2\right]}dt$$
$$+ \int_0^{T^{(\mathrm{F})}} \frac{\sqrt{T^{(\mathrm{F})}} e^{j\pi t\left(c_n+\frac{(1-\alpha)}{T^{(\mathrm{F})}}\right)}}{j2t\pi\left[1-\left(\frac{4\alpha t}{T^{(\mathrm{F})}}\right)^2\right]}dt - \int_0^{T^{(\mathrm{F})}} \frac{\sqrt{T^{(\mathrm{F})}} e^{j\pi t\left(c_n-\frac{(1-\alpha)}{T^{(\mathrm{F})}}\right)}}{j2t\pi\left[1-\left(\frac{4\alpha t}{T^{(\mathrm{F})}}\right)^2\right]}dt$$
$$\triangleq \mathcal{I}_1+\mathcal{I}_2+\mathcal{I}_3-\mathcal{I}_4. \tag{A.2}$$

Utilizing [16, 01.03.21.0140.01] in (A.2), we get (15). Similarly utilizing [16, 01.03.21.0141.01] in (A.2), we get (16).

B. Proof of Lemma 2

The basis function defined in (18) decomposes the received undesired FSS broadcast signal interference at the NR receiver as

$$I_n[\ell] = \frac{\mathcal{A}_4}{\sqrt{T_u^{(\mathrm{N})}}} \int_{\mathbb{R}} \sum_{k=0}^{K-1} \sum_{i=1}^{L} a_k h_i^{(\mathrm{N})} e^{j2\pi d_n t}\, p(t-G_k) \prod\left(\frac{t-\ell T^{(\mathrm{N})}}{T_s^{(\mathrm{N})}}\right) dt, \tag{B.1}$$

where $\mathcal{A}_4 = \sqrt{g_T^{(\mathrm{F})}\,\hat{g}_R^{(\mathrm{N})}\,P_T^{(\mathrm{F})}}$ and $d_n = \Delta f_{\mathrm{off}}^{(\mathrm{F})} - n/T_s^{(\mathrm{N})}$, and $G_k = kT^{(\mathrm{F})} - \tau_k^{(\mathrm{F})} - \theta^{(\mathrm{F})}$. Since NR symbol duration is not a multiple of the DVB-S2 symbol duration, the number of DVB-S2 symbols interfering entirely over the NR symbol is approximately $\lfloor\xi\rfloor$ which are: $a_k, a_{k+1}, a_{k+2,\cdots,a_{\lfloor\xi\rfloor-1}}$. For the sake of simplicity, we ignore $(k-1)$-th and $\lfloor\xi\rfloor$-th symbols that interfere partially respectively at the beginning and the end of NR symbol. Utilizing the above discussion, the interference at the NR receiver can be expressed by substituting (2) in (B.1) as

$$I_n[\ell] = \frac{\mathcal{A}_4}{\sqrt{T_u^{(\mathrm{N})}}} \sum_{b=0}^{\lfloor\xi\rfloor-1} a_{k+b} \sum_{i=1}^{L} h_i^{(\mathrm{F})} \mathcal{J}, \tag{B.2}$$

where $\mathcal{J}$ is defined in (B.3). Utilizing [16, 01.03.21.0144.01] in (B.3), we get (22) and (23). Similarly utilizing [16, 01.03.21.0145.01] in (A.2), we get (24) and (25).

REFERENCES

[1] A. Al-Jumaily, A. Sali, V. P. G. Jiménez, F. P. Fontán, M. J. Singh, A. Ismail, Q. Al-Maatouk, A. M. Al-Saegh, and D. Al-Jumeily, "Evaluation of 5G coexistence and interference signals in the C-Band satellite earth station," *IEEE Trans. Veh. Technol.*, vol. 71, no. 6, pp. 6189–6200, Mar. 2022.

[2] "Sharing studies between IMT-Advanced systems and geostationary satellite networks in the fixed-satellite service in the 3 400-4 200 and 4 500-4 800 MHz frequency bands," Rep. ITU-R M.2109, 2007. [Online]. Available: itu.int/dms_pub/itu-r/opb/rep/R-REP-M.2109-2007-PDF-E.pdf

[3] L. C. Alexandre, L. de Oliveira Veiga, A. Linhares, J. R. P. Moreira, M. Abreu, and A. C. S. Junior, "Coexistence analysis between 5G NR and TVRO in C-band," *J. Commun. Inf. Syst.*, vol. 35, no. 1, pp. 198–202, Jul. 2020.

[4] L. C. Alexandre, L. O. Veiga, A. Linhares, H. R. D. Filgueiras, and A. Cerqueira, "Technological solution for enabling 5G NR and TVRO peaceful coexistence in C-band," in *European Conference on Antennas and Propagation (EuCAP)*. IEEE, 2021, pp. 1–5.

[5] E. Lagunas, C. G. Tsinos, S. K. Sharma, and S. Chatzinotas, "5G cellular and fixed satellite service spectrum coexistence in C-Band," *IEEE Access*, vol. 8, pp. 72 078–72 094, 2020.

[6] B. Lim and M. Vu, "Interference analysis for coexistence of terrestrial networks with satellite services," *IEEE Trans. Wireless Commun.*, Aug. 2023.

[7] Z. Li, S. Han, L. Xiao, and M. Peng, "Cooperative non-orthogonal broadcast and unicast transmission for integrated satellite-terrestrial network," *IEEE Trans. Broadcast.*, Dec. 2023.

[8] L. Yin and B. Clerckx, "Rate-splitting multiple access for satellite-terrestrial integrated networks: Benefits of coordination and cooperation," *IEEE Trans. Wireless Commun.*, vol. 22, no. 1, pp. 317–332, Jul. 2022.

[9] M. Rice, *Digital Communications: A Discrete-time Approach*, 1st ed. Pearson, 2008.

[10] A. Thakur, S. De, and G.-M. Muntean, "Co-channel secondary deployment over DTV bands using reconfigurable radios," *IEEE Trans. Veh. Technol.*, vol. 69, no. 10, pp. 12 202–12 215, Aug. 2020.

[11] "Reference radiation pattern for earth station antennas in the fixed-satellite service for use in coordination and interference assessment in the frequency range from 2 to 31 GHz," Rec. ITU-R S.465-6, S Series, Fixed-satellite service, Jan. 2010.

[12] "Attenuation by atmospheric gases and related effects," Rec. ITU-R P.676-13, P Series, Radiowave propagation, Aug. 2022. [Online]. Available: itu.int/rec/R-REC-P.676-13-202208-I/en

[13] "5G: Study on channel model for frequencies from 0.5 to 100 GHz," 3GPP TR 38.901 ver. 16.1.0 Rel. 16, Nov. 2020.

[14] A. Morello and V. Mignone, "DVB-S2: The second generation standard for satellite broad-band services," *Proc. IEEE*, vol. 94, no. 1, pp. 210–227, Jan. 2006.

[15] "5G; NR; base station (BS) radio transmission and reception," 3GPP TS 38.104 ver. 16.4.0 Rel. 16, Jul. 2020.

[16] Wolfram, "The wolfram functions site." [Online]. Available: functions.wolfram.com